Lossless, Multiband, on Board, Compression of Hyperspectral Images

Bruno Carpentieri, Raffaele Pizzolante

Abstract— Hyperspectral remote sensing produces a huge amount of three-dimensional digital data: the hyperspectral images. Hyperspectral images are used to recognize objects and to classify materials on the surface of the earth. They are considered a useful tool in different real-life applications. In this paper we propose a novel approach for the efficient lossless compression of hyperspectral images, which is based on a predictive coding model. Our approach relies on a three-dimensional predictive structure that uses, one or more, previous bands as references to exploit the redundancies among the third dimension. The proposed technique uses limited resources in terms of CPU and memory usage. The achieved results are comparable, and often better, with respect to the other state-of-art lossless compression techniques for hyperspectral images.

Keywords— Hyperspectral images, lossless compression, low complexity, 3-D data.

I. Introduction

THREE-dimensional data generated by hyperspectral remote sensing are collected from the visible and the near-infrared spectrum of reflected light. The human visual system, can only see visible light: the wavelengths between 360 to 760 nanometers (nm), the hyperspectral data, commonly referred as hyperspectral images, reveal also the frequencies of ultraviolet and infrared rays. Thus, a hyperspectral image is a collection of information derived from the electromagnetic spectrum of an observed area.

Figure 1 shows a graphical representation of an hyperspectral image that highlights its three-dimensional nature. The X-axis indicates the columns, the Y-axis indicates the rows and the Z-axis indicates the spectral channels of the hyperspectral image, often referred as bands.

There are many real-life applications in which hyperspectral data are used: agriculture, mineralogy, physics, surveillance, etc.. In geological applications, for example, the capabilities of hyperspectral remote sensing can be useful to identify various types of minerals, by permitting the search of minerals and oil.

Each hyperspectral sensor generates daily data in the order of many gigabytes, it is therefore necessary to compress these data so to be able to transmit and to store them efficiently. Lossless compression is generally used in order to preserve the original data, because of the high costs involved in the acquisitions and also for the importance of these data in delicate tasks (as for instance target classification or detection).

In this paper, we propose a novel technique for the lossless compression of hyperspectral images. The proposed algorithm is based on the predictive coding model and the proposed predictive structure uses a multiband three-dimensional structure. Our technique allows to customize the encoding parameters, as for instance the number of the previous bands which will be used as references. We designed our approach to optimize the computational complexity and the memory usage, which depends on the chosen parameters.

The experimental results show that the compression results obtained by this algorithm reach, and often outperform, the performance of the other state of the art approaches, and that the algorithm maintains a good trade-off between computational complexity/memory usage and compression performances.

Our algorithm is suitable for on board implementations: it is highly configurable and it is possible to implement it with limited hardware capabilities, as on airplane or a satellite.

The paper is organized as follow: Section 2 shortly discusses previous work on lossless and lossy compression of hyperspectral images, Section 3 describes the proposed lossless compression approach, Section 4 reports the experimental results and Section 5 highlights our conclusion and future work directions.

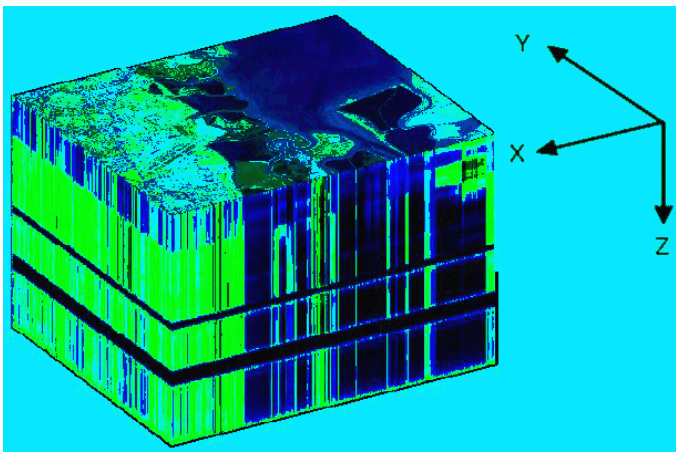

Figure 1. Graphical representation of an hyperspectral image (NASA AVIRIS Moffett Field).

B. Carpentieri and R. Pizzolante are with the Dipartimento di Informatica, Università di Salerno, I-84084 Fisciano (SA) – Italia. (phone: +39 089969500; fax: +39 089969600/1; e-mail: bc@dia.unisa.it , rpizzolante@unisa.it).

II. Previous Work

Lossless compression of hyperspectral images is generally based on the predictive coding model. The predictive-based approaches have different advantages: they use limited resources in terms of computational power and memory and achieve good compression performances. Thus, these models are suitable for on board implementations.

Spectral-oriented Least SQuares (SLSQ) [20], Linear Predictor (LP) [20], Fast Lossless (FL) [8], CALIC-3D [10], M-CALIC [10] and EMPORDA [21] are among the state-of-art predictive-based techniques.

Other approaches are designed for offline compression, since they use more sophisticated techniques and/or require to have available at once the whole hyperspectral image. These approaches are not suitable for an on board implementation but can achieve better compression performances.

Mielikainen, in [12], proposed an approach for the compression of hyperspectral image through Look-Up Table (LUT). LUT predicts each pixel by using all the pixels in the current and in the previous band, by searching the nearest neighbor, in the previous band, which has the same pixel value as the pixel located in the same spatial coordinates as the current pixel. LUT has high compression performances, but it uses more resources in terms of memory and CPU usage.

Other lossless techniques are based on dimensionality reduction through principal component transform [17].

An error-resilient lossless compression technique is proposed in [1].

For the lossy compression of hyperspectral images, the compression algorithms are, generally, based on 3D frequency transforms: as for examples 3-D Discrete Wavelet Transform (3D-DWT) [9], 3-D Discrete Cosine Transform (3D-DCT) [11], Karhunen–Loève transform (KLT) [16], etc.. These approaches are easily scalable. On the other hand, they require to maintain in memory the entire hyperspectral image at the same time. Locally optimal Partitioned Vector Quantization (LPVQ) [3, 13] applies a Partitioned Vector Quantization (PVQ) scheme independently to each pixel of the hyperspectral image. The variable sizes of the partitions are chosen adaptively and the indices are entropy coded. The codebook is included as part of the coded output.

This technique can be used also in lossless mode, but the high costs required in terms of CPU and memory do not allow an on board implementation

III. Multiband Compression of Hyperspectral Images

Hyperspectral images present a strong correlation among consecutive bands (inter-band) and a high correlation in the spatial context (intra-band).

Figure 2 highlights the correlation among consecutive bands: the X-axis indicates the bands and the Y-axis indicates the Pearson's correlation [15] between the i-th band and the (i-1)-th band. As it is possible to observe, the Pearson's correlation assumes high values in most of the cases.

These characteristics can be exploited by a compression

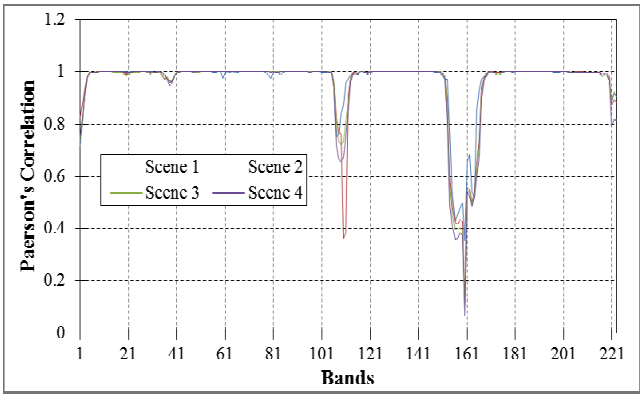

Figure 2. Pearson's correlation among consecutive bands for the fourth scenes of the Moffett Field hyperspectral image.

algorithm that optimizes the redundancy among the third dimension.

The proposed lossless compression technique: named Lossless MultiBand compression for Hyperspectral Images (LMBHI), is based on the predictive coding model.

LMBHI takes as input the hyperspectral image, and, for each pixel X of the hyperspectral image performs the prediction of the current pixel, $\hat{X}$, by using the appropriate prediction context of X.

Since the pixels of the first band have no reference pixels in the previous bands, they are predicted by using a bi-dimensional predictive structure: the 2-D Linearized Median Predictor (2-D LMP) [19] that uses only the neighboring pixels.

All the other pixels of all the other bands are predicted by using a new three-dimensional predictive approach, which uses for the prediction the neighboring pixels of X and its reference pixels in the previous bands.

After the prediction step, the prediction error:

$$e = \left\lfloor X - \hat{X} \right\rfloor$$

is computed, modeled, and coded.

In the following, we give more details on all the components of the algorithm.

The 2-Dimensional Linearized Median Predictor (2D-LMP) [19] uses as prediction context the three neighboring pixels of X, referred as I_A, I_B and I_C, as shown in Figure 3.

The predictive structure is derived from the well-established 2-D Median Predictor, that is used in JPEG-LS [4].

I_C	I_B
I_A	X

Figure 3. The prediction context of the 2D-LMP predictive structure. The gray part is already coded and the white part is not coded yet.

ISBN: 978-1-61804-285-9

The 2-D Median Predictor has the following predictive structure:

$$\hat{X} = \begin{cases} \max(I_A, I_B) & if \quad I_C \geq \min(I_A, I_B) \\ \min(I_A, I_B) & if \quad I_C \leq \max(I_A, I_B) \\ I_A + I_B - I_C & otherwise \end{cases}$$

Median Predictor selects one of the above three options, depending on the context.

By combining all the three options, it is possible to obtain the predictive structure of 2D-LMP, defined as:

$$\hat{X} = \frac{2 \cdot (I_A + I_B)}{3} - \frac{I_C}{3}$$

Our three-dimensional Multiband Linear Predictor (3D-MBLP) uses, instead, N (up to 16) neighboring pixels (of X) for each of the B previous bands, to compute the prediction of X.

In order to define the prediction context, we need to enumerate the neighboring pixels of X in the current and in the previous bands.

For these reasons, we define an enumeration that depends on a distance d, defined as:

$$d((z,u,v),(z,w,z)) = \sqrt{(u-w)^2 + (v-z)^2}$$

When more pixels have the same indices, it is possible to reassign the indices of these pixels in clockwise order with respect to X.

Let $I_{i,j}$ denotes the i-th pixel of the j-th band, according to the above enumeration.

Let $I_{0,j}$ denotes the pixel that has the same spatial coordinates of X, of the j-th band ($j \neq k$), according to the above enumeration.

Figure 4 shows the resulting enumeration of the first N=16 pixels for the k-th band.

3D-MBLP is based on least squares optimizations and the prediction is computed as:

$$\hat{X} = \sum_{i=1}^{B} \alpha_i \cdot I_{0,k-i}$$

The coefficients:

$$\alpha_0 = [\alpha_1 \quad \cdots \quad \alpha_B]^T$$

are chosen to minimize the energy of the prediction error

$$P = \sum_{i=1}^{N} \left(I_{i,k} - \hat{I}_{i,k} \right)^2$$

P can be rewritten in matrix notation as: $P = (\boldsymbol{C}\alpha - \boldsymbol{X})^T \cdot (\boldsymbol{C}\alpha - \boldsymbol{X})$, where:

$$\boldsymbol{C} = \begin{bmatrix} I_{1,k-1} & \cdots & I_{1,k-B} \\ \vdots & \ddots & \vdots \\ I_{N,k-1} & \cdots & I_{N,k-B} \end{bmatrix} \text{ and } \boldsymbol{X} = \begin{bmatrix} I_{1,k} \\ \vdots \\ I_{N,k} \end{bmatrix}.$$

By taking the derivate of P and by setting it to zero, we obtain the optimal coefficients:

$$(\boldsymbol{C}^T\boldsymbol{C})\ \alpha_0 = (\boldsymbol{C}^T\boldsymbol{X}). \quad (1)$$

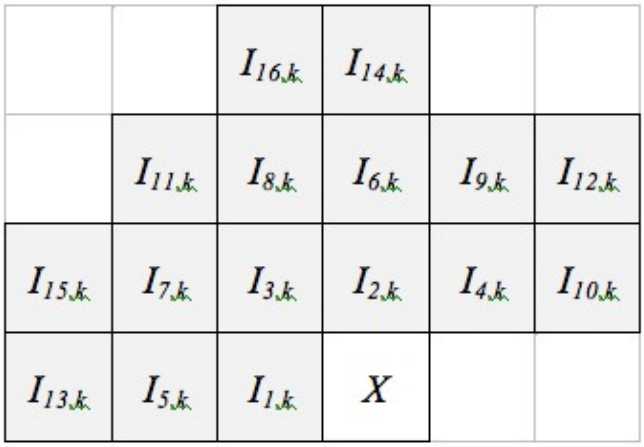

Figure 4. The prediction context (N=16) for the current pixel X in the k-th band. The gray pixels have already been coded, the white pixels are not coded yet.

Once the coefficients α_0, which solve the linear system (1), are obtained, then it is possible to compute the prediction $\hat{X}$ of the current pixel X.

A prediction error can assume positive or negative values. In order to have only non-negative values, similarly to [14], we mapped each prediction error with an invertible mapping function M (which does not alter the redundancy among the errors). The simplified definition of the function M is:

$$M(error) = \begin{cases} 2|error| & if \quad error \geq 0 \\ 2|error| - 1 & otherwise \end{cases}$$

where $|x|$ means the absolute value of x.

Once mapped, the error is coded through arithmetic coding.

The main computational costs of our approach are due to the resolution of the linear system (1) to generate the optimal coefficients α_0 for the computation of the predicted pixel. By using the normal equation method, the linear system (1) can be solved with $(N + B/3) \cdot B^2$ floating-point operations [6].

Figure 5 shows the trend of the computational complexity of our predictive model, in terms of number of operations (Y-axis) that are required for the solving of the linear system (1), by using configurations with different parameters (X-axis).

If we use only the previous band as a reference (B = 1), only about 20 operations are needed to solve the system.

Instead 4 or 9 times more operations are required, if we use two previous bands (B = 2) or three previous bands (B = 3).

A linear system can have three kinds of solutions: no solutions, one solution and infinity solutions.

In the first and the third scenarios, the proposed predictive structure cannot perform the prediction.

In these cases, it is desirable to use another low-complexity predictive structure and we have used the 3-D

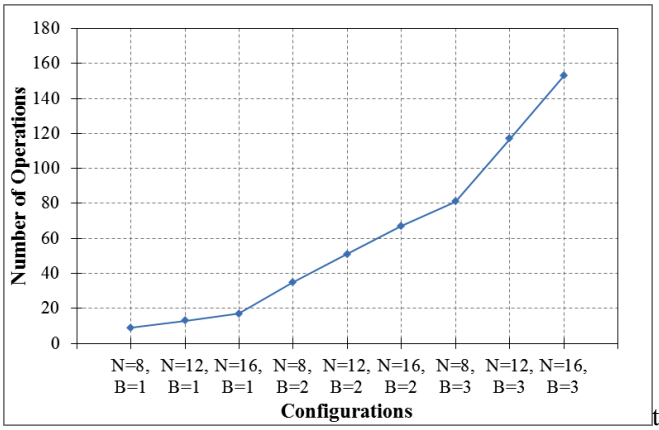

Figure 5. The number of operations (*Y*-axis) required to solve the linear system (1), by using different parameters (*X*-axis).

Distances-based Linearized Median Predictor (3D-DLMP) [19].

IV. Experimental Results

We have experimentally tested our approach on five Airborne Visible/Infrared Imaging Spectrometer (AVIRIS) [2] hyperspectral images provided by the NASA Jet Propulsion Lab (JPL) [7], each image is subdivided into scenes.

The test set we have used is composed by the following images: Lunar Lake, Moffett Field, Jasper Ridge, Cuprite and Low Altitude, respectively of 3, 4, 6, 5 and 8 scenes. Except for the last scenes of each image that have a minor number of rows, each scene of the images has 614 columns, 512 lines and 224 spectral bands. Each sample is represented by an integer with 16 bits.

Table 1 reports the results achieved by using our approach with different parameters on all the test images. These results are reported in terms of compression ratio (C.R.) and they are compared with other state of the art lossless compression schemes.

By using two previous bands as references (B = 2), LMBHI outperforms, in average, all the state of the art approaches.

By using only the previous band as reference (B = 1), LMBHI outperforms all the state of the art techniques, with exception of LPVQ: an algorithm that is not suitable for on board implementation.

In this latter case, LMBHI achieves better results with respect to LPVQ on 3 of the 5 hyperspectral images: Moffett Field, Jasper Ridge and Low Altitude, but LPVQ gains on Cuprite and especially on Lunar Lake.

The high flexibility and adaptability of our approach makes it considerable for on board implementations. In fact, the coding parameters can be customized depending on the hardware available.

Therefore, it is possible to implement the algorithm on different typologies of sensors, by using an appropriate configuration for each one. Moreover, the proposed approach could be easily scaled for future generation sensors, which will have better hardware capabilities.

Methods / Images	Lunar Lake	Moffett Field	Jasper Ridge	Cuprite	Low Altitude	*Average*
LMBHI (*N*=16, *B*=2)	3.27	3.23	3.23	3.27	3.07	*3.21*
LMBHI (*N*=8, *B*=2)	3.21	3.18	3.18	3.21	3.02	*3.16*
LMBHI *(N=8, B=1)*	3.18	3.14	3.16	3.19	2.99	*3.13*
LPVQ	3.31	3.01	3.12	3.27	2.97	*3.14*
SLSQ	3.15	3.14	3.15	3.15	2.98	*3.11*
JPEG-2000	2.98	2.99	2.96	2.98	2.82	*2.95*
LP	3.05	2.88	2.94	3.03	2.76	*2.93*
JPEG-LS	2.87	2.90	2.87	2.87	2.74	*2.85*
Diff. JPEG2000	2.94	2.83	2.82	2.92	2.69	*2.84*
Diff. JPEG-LS	2.93	2.84	2.81	2.91	2.70	*2.84*
M-CALIC	3.19	3.27	3.06	3.14	N.A.	*N.A.*
CALIC-3D	3.06	3.08	3.09	3.25	N.A.	*N.A.*
LUT	3.44	3.23	3.40	3.17	N.A.	*N.A.*

Table 1. Compression results (C.R.) achieved by LMBHI (by using various parameter configurations), compared to other lossless compression methods.

V. Conclusions and Future Work

In this paper we have proposed a predictive-based scheme to compress hyperspectral images, which uses a multiband three-dimensional predictive structure and that it is suitable for onboard implementations.

The results achieved are comparable and often outperform the other state of the art lossless compression techniques.

Future work will include a more intensive testing of the proposed approach, by taking also into consideration the possibility of pre-processing the hyperspectral image before compression, or by reordering the bands by considering their correlation.

This will possibly improve the compression performance [5, 13, 18].

Acknowledgment

The authors would like to thank our students Dario Di Nucci, Fabio Palomba, Stefano Ricchiuti and Michele Tufano for testing a preliminary version of our algorithm.

References

[1] A. Abrando, M. Barni, E. Magli, F. Nencini, "Error-Resilient and Low-Complexity Onboard Lossless Compression of Hyperspectral Images by Means of Distributed Source Coding", IEEE Trans. on Geosci., vol. 48, no. 4, pp. 1892-1904, April, 2010.

[2] AVIRIS NASA Page, Available on: http://aviris.jpl.nasa.gov/, Accessed on Oct. 2013.

[3] B. Carpentieri, J.A. Storer, G. Motta, F. Rizzo, "Compression of Hyperspectral Imagery", Proceedings of IEEE Data Compression Conference (DCC '03), Snowbird, UT, USA, pp. 317–324, 25–27 March 2003.

[4] B. Carpentieri, M. Weinberger, G. Seroussi, "Lossless Compression of Continuous Tone Images", Proceeding of IEEE, vol. 88, no. 11, pp. 1797-1809, November, 2000.

[5] B. Carpentieri, "Hyperpectral Images: Compression, Visualization and Band Ordering", Proceedings of IPCV 2011; Volume 2, pp. 1023–1029, 2011.

[6] G.H. Golub, C.F. Van Loan, “Matrix Computations, 3rd ed. Baltimore”, MD: The Johns Hopkins Univ. Press, 1996.
[7] Jet Propulsion Laboratory (JPL) Page, Available on: http://www.jpl.nasa.gov/. Accessed on Oct. 2013.
[8] M. Klimesh, “Low-complexity lossless compression of hyperspectral imagery via adaptive filtering”, IPN Progress Report, vol. 42-163, pp. 1–10, 2005.
[9] S. Lim, K. Sohn, C. Lee, “Compression for hyperspectral images using three dimensional wavelet transform,” in Proc. IGARSS, Sydney, Australia, 2001, pp. 109–111.
[10] E. Magli, G. Olmo, E. Quacchio, "Optimized onboard lossless and near-lossless compression of hyperspectral data using CALIC", Geoscience and Remote Sensing Letters, IEEE , vol.1, no.1, pp.21,25, Jan. 2004.
[11] D. Markman, D. Malah, “Hyperspectral image coding using 3D transforms,” Proc. IEEE ICIP, Thessaloniki, Greece, pp. 114–117, 2001.
[12] J. Mielikainen , “Lossless compression of hyperspectral images using lookup tables”, IEEE Signal Process. Letters, vol. 13, no. 3, pp. 157–160, Mar. 2006.
[13] G. Motta, F. Rizzo, J.A. Storer, Hyperspectral Data Compression, Springer Science, Berlin, Germany, 2006.
[14] G. Motta, J.A. Storer, B. Carpentieri, “Lossless Image Coding via Adaptive Linear Prediction and Classification”, Proceedings of the IEEE, vol. 88, no. 11, pp. 1790–1796, November, 2000.
[15] K. Pearson, “Mathematical contributions to the theory of evolution.-III. Regression, heredity and panmixia. Philos.”, Trans. R. Soc. Lond., 187, pp. 253–318, 1896.
[16] B. Penna, T. Tillo, E. Magli, G. Olmo, “Transform Coding Techniques for Lossy Hyperspectral Data Compression”, IEEE Trans. on Geosci., vol. 45, no. 5, pp. 1408-1421, May, 2007.
[17] M. Pickering, M. Ryan, “Efficient spatial-spectral compression of hyperspectral data”, IEEE Trans. Geosci. Remote Sens., vol. 39, no. 7, pp. 1536–1539, Jul. 2001.
[18] R. Pizzolante, B. Carpentieri, “Visualization, Band Ordering and Compression of Hyperspectral Images”, Algorithms, 5(1), pp. 76-97, 2012.
[19] R. Pizzolante, B. Carpentieri, "Lossless, low-complexity, compression of three-dimensional volumetric medical images via linear prediction", International Conference on Digital Signal Processing (DSP) 2013 18th, pp.1,6, 1-3 July 2013.
[20] F. Rizzo, B. Carpentieri, G. Motta, J..A. Storer, "Low-complexity lossless compression of hyperspectral imagery via linear prediction", Signal Processing Letters, IEEE , vol.12, no.2, pp. 138,141, Feb. 2005.
[21] J.E. Sánchez, E. Auge, J. Santaló, I. Blanes, J. Serra-Sagristà, A.B. Kiely, “Review and Implementation of the Emerging CCSDS Recommended Standard for Multispectral and Hyperspectral Lossless Image Coding”, Proceedings of 2011 First International Conference on Data Compression, Communications and Processing (CCP), Palinuro, Italy, pp. 222–228, 21–24 June 2011.